Received: 27 March 2020 | Revised: 7 July 2020 | Accepted: 13 July 2020

DOI: 10.1096/fj.202000603R

RESEARCH ARTICLE

THE FASEB JOURNAL

RNA-Seq analysis on *ets1* mutant embryos of *Xenopus tropicalis* identifies *microseminoprotein beta gene 3* as an essential regulator of neural crest migration

Chengdong Wang[1] | Xufeng Qi[2] | Xiang Zhou[3] | Jianmin Sun[4] | Dongqing Cai[2] | Gang Lu[1] | Xiongfong Chen[5] | Zhihua Jiang[6] | Yong-Gang Yao[7,8,9] | Wai Yee Chan[1,9,10] | Hui Zhao[1,9,10]

[1]Key Laboratory for Regenerative Medicine, Ministry of Education, School of Biomedical Sciences, Faculty of Medicine, The Chinese University of Hong Kong, Hong Kong SAR, China

[2]Key Laboratory of Regenerative Medicine of Ministry of Education, Department of Developmental & Regenerative Biology, Jinan University, Guangzhou, China

[3]Key Laboratory of Agricultural Animal Genetics, Breeding, and Reproduction of Ministry of Education, College of Animal Science and Technology, Huazhong Agricultural University, Wuhan, P.R. China

[4]Department of Pathogen Biology and Immunology, School of Basic Medical Sciences, Ningxia Medical University, Yinchuan, China

[5]Advanced Biomedical Computing Center, National Cancer Institute, National Institutes of Health, Frederick, MD, USA

[6]Department of Animal Sciences and Center for Reproductive Biology, Washington State University, Pullman, WA, USA

[7]Key Laboratory of Animal Models and Human Disease Mechanisms of the Chinese Academy of Sciences & Yunnan Province, Kunming Institute of Zoology, Chinese Academy of Sciences, Kunming, China

[8]Kunming College of Life Science, University of Chinese Academy of Sciences, Kunming, China

[9]Kunming Institute of Zoology - The Chinese University of Hong Kong (KIZ-CUHK) Joint Laboratory of Bioresources and Molecular Research of Common Diseases

[10]Hong Kong Branch of CAS Center for Excellence in Animal Evolution and Genetics, The Chinese University of Hong Kong, Hong Kong SAR, China

Correspondence
Hui Zhao, Key Laboratory for Regenerative Medicine, Ministry of Education, School of Biomedical Sciences, Faculty of Medicine, The Chinese University of Hong Kong, Room 620A, LKS Integrated Biomedical Sciences Building, Hong Kong SAR, China.
Email: zhaohui@cuhk.edu.hk

Funding information
Ministry of Science and Technology of China, Grant/Award Number: 2016YFE0204700; Research Grants Council, University Grants Committee (RGC, UGC), Grant/Award Number:

Abstract

The proto-oncogene *ets1* is highly expressed in the pre-migratory and migratory neural crest (NC), and has been implicated in the delamination and migration of the NC cells. To identify the downstream target genes of Ets1 in this process, we did RNA sequencing (RNA-Seq) on wild-type and *ets1* mutant *X. tropicalis* embryos. A list of genes with significantly differential expression was obtained by analyzing the RNA-Seq data. We validated the RNA-Seq data by quantitative PCR, and examined the expression pattern of the genes identified from this assay with whole mount in situ hybridization. A majority of the identified genes showed expression in migrating NC. Among them, the expression of *microseminoprotein beta gene 3* (*msmb3*) was

Abbreviations: BMP, bone morphogenic protein; ChIP, chromatin immunoprecipitation; CRISPR, clustered regularly interspaced short palindromic repeats; DEG, differently expressed gene; EMT, epithelial-to-mesenchymal transition; MO, antisense morpholino oligonucleotides; NC, neural crest; PCR, polymerase chain reaction; qPCR, quantitative RT-PCR; RNA-Seq, RNA sequencing; RPKM, reads per kilo base per million; RPM, reads per million; RT-PCR, reverse-transcription polymerase chain reaction; sgRNA, single guide RNA; TALEN, transcription activator-like effector nucleases; WMISH, whole mount in situ hybridization; WT, wild-type.

14167017 and 14112618; Bureau of International Cooperation, Chinese Academy of Sciences, Grant/Award Number: 152453KYSB20170031

positively regulated by Ets1 in both *X. laevis* and *X. tropicalis*. Knockdown of *msmb3* with antisense morpholino oligonucleotides or disruption of *msmb3* by CRISPR/Cas9 both impaired the migratory streams of NC. Our study identified *msmb3* as an Ets1 target gene and uncovered its function in maintaining neural crest migration pattern.

KEYWORDS

cell migration, Ets1, Msmb3, neural crest

1 | INTRODUCTION

The proto-oncogene Ets1 belongs to the ETS family of transcription factors that share a unique DNA binding domain, the Ets domain.[1] Depending on the partners it binds, Ets1 can function as either transcriptional activator or repressor.[2,3] Ets1 is widely involved in many biological processes during embryonic development, one of which is the neural crest (NC) development.[2,4]

The NC is a multipotent population of cells found only in vertebrate, and contributes to a large variety of tissues, such as melanocytes, cranial bone and cartilage, and neurons and glia in the peripheral nervous system. The NC is induced and specified at the neural plate border region. After specification, the NC cells undergo epithelial-to-mesenchymal transition (EMT), leave its original territory and migrate throughout the embryo. *Ets1* is expressed in pre-migratory and migratory NC during chicken and *Xenopus* embryogenesis.[3,5] In chicken embryos, Ets1 plays essential roles in cranial NC delamination and cooperates with Snail2 to provoke EMT.[6] In *Xenopus* embryos, knockdown of *ets1* blocked NC migration, but did not obviously affect NC formation.[3] In contrast, overexpression of *ets1* represses NC formation by physical interaction with Hdac1 to attenuate the outputs of BMP signaling epigenetically.[3] Knockout of *Ets1* in mice caused perinatal lethality due to heart defects. Further study revealed a ventricular septal defect in *Ets1* knockout mice that is caused by the interfered migration of cardiac NC to the proximal outflow tract.[7]

Ets1 is also implicated in heart development through regulating heart mesoderm specification. Targeted knockdown of *ets1* in *Xenopus* heart mesoderm caused delayed formation of the primitive heart tube and depleted endocardial tissue.[8] The requirement of Ets1 for endocardium formation may be explained by a previous report that a *Gata4* enhancer regulated by ETS proteins was active predominately in mouse endocardium.[9] Knockout of both *Ets1* and *Ets2* in mice caused striking defects in vascular branching, indicating essential roles of Ets1 and Ets2 in embryonic angiogenesis.[10] Ets1 is essential during hematopoiesis as well. Downregulation of *Ets1* is required for erythroid differentiation.[11] Ets1 also binds to the promoter of chicken *Gata1*, an erythroid specific transcription factor.[12] Indeed, Ets1 exerts functions in the differentiation of all lymphoid cells.[13] Studies in *Ets1* knockout mice showed that Ets1 is important for the development and function of B cells, T cells, and natural killer (NK) cells.[14]

Although Ets1 plays important roles in the NC development, formation of heart and blood vessel, and hematopoiesis system, the knowledge about Ets1 downstream target genes and underlying mechanism as to how Ets1 regulates these genes during embryonic development are largely unknown. We previously generated *X tropicalis* mutant line harboring *ets1* mutation with transcription activator-like effector nuclease (TALEN).[15] RNA-Seq analysis was performed on wild-type and *ets1* mutant embryos at mid-neurula stages, and identified a list of differentially expressed genes (DEGs). The changes in their expression were further confirmed by quantitative RT-PCR. Several identified DEGs were expressed in migrating NC, including the *microseminoprotein beta, gene 3* (*msmb3*). We further showed that Ets1 is sufficient and necessary for inducing *msmb3* expression, and *msmb3* is required to maintain NC migration patterns.

2 | MATERIALS AND METHODS

2.1 | Explant dissection and sample preparation

Natural mating was performed between two heterozygous *ets1* mutant frogs. When the offspring developed to stage 17, the posterior portion of the embryo was dissected for genomic DNA extraction using the extraction kit (Favorgen Biotech Corp), and the remaining part was stored in TRIzol. For genotyping, allele specific PCR was performed using primers specifically targeting wild-type or mutant allele (Table S2). The results were then confirmed by sequencing. Then, the remaining parts of embryos with the same genotype were pooled for RNA extraction. Two batches of RNA samples were separately extracted from wild-type and homozygous *ets1* mutant embryos, and were sent to do RNA sequencing.

2.2 | RNA-Seq and data analysis

The quality of the total RNA was assessed using the Agilent 2100 Bioanalyzer. After library construction, sequencing

was performed using Illumina Hiseq 2500 platform by the BGI Tech Solutions (Hong Kong) Co. Limited. Clean data (4G) were obtained for each sample. *X tropicalis* genome v9.1[16] and the annotation file were downloaded from the NCBI (https://www.ncbi.nlm.nih.gov/genome?term=xenopus%20tropicalis). After reads quality and length trimming, CLC Genomics Workbench, v10.0.1 (CLC bio, a QIAGEN company, Boston, MA, USA) was used to process RNA-Seq data for read mapping and gene expression quantification. Read mapping parameters were set to 95% similarity, 90% length coverage, and maximum number of two mismatches. Expression of each gene was quantified as raw count of mapped reads or adjusted as reads per million (RPM) or reads per kilo base per million (RPKM) mapped reads. The edgeR program[17] was used to identify differently expressed genes between wild-type and *ets1* mutant embryos. In the present study, genes with fold change greater than or equal to 2 and *P* value less than 0.05 were selected as significant differently expressed genes (DEGs).

2.3 | DNA constructs

The gene fragments of the 13 DEGs examined by WMISH were amplified using PCR and subcloned into pBluescript II KS (+) vector. The open reading frame of *X. tropicalis msmb3* was subcloned into pCS2$^+$ vector. For construction of sgRNA expression vector, two oligonucleotides containing target sequence were annealed and integrated into DR274 vector. All vectors were verified by sequencing. The primers are listed in Table S2.

2.4 | Microinjection, LacZ staining, and whole mount in situ hybridization

X. laevis embryos were obtained by in vitro fertilization and cultured as previously described.[18] *X. tropicalis* embryos were obtained by natural mating and cultured following the Harland *X. tropicalis* website (https://tropicalis.berkeley.edu/index.html). Embryos were staged according to Nieuwkoop and Faber.[19] Capped mRNAs were synthesized in vitro using the mMessage mMachine kit (Thermo Fisher Scientific) and the sgRNA was transcribed with MAXIscript T7 in vitro transcription kit (Thermo Fisher Scientific). After synthesis, both were purified using RNeasy MinElute Cleanup Kit (Qiagen). Cas9 protein was purchased from PNA Bio INC. Translation-blocking MOs were purchased from Gene Tools, inc. (ets1MO, 5′-TGAGATCTAGCGCAGCTTTCATGGC-3′; msmb3LMO, 5′-TTATGCTTGAAGTTGTTGCAGACAC-3′). LacZ staining was performed using X-Gal as described previously.[18] Whole mount in situ hybridization was performed according to the standard protocol.[20] The digoxigenin-labeled antisense RNA probes were synthesized with T7 or T3 RNA polymerase (Roche) using linearized templates.

2.5 | Chromatin immunoprecipitation

Chromatin immunoprecipitation (ChIP) assay using *Xenopus* embryos was performed following the published protocols.[21] Briefly, *ets1-FLAG* mRNA was injected into *X. laevis* embryos at two-cell stage. The injected embryos were collected at stage 17 for cross-linking with 1% of formaldehyde. After shearing the chromatin by sonication, immunoprecipitation was done using anti-FLAG antibody (Sigma-Aldrich). The immunoprecipitated DNA fragments were purified and analyzed by PCR using primers listed in Table S2.

2.6 | RNA extraction, RT-PCR, and quantitative PCR

Total RNA was extracted from *Xenopus* embryos using the TRIzol reagent (Invitrogen) and purified with RNeasy MinElute Cleanup Kit (Qiagen), and cDNA was synthesized using Superscript III (Thermo Fisher Scientific) according to the manufacturer's instruction. Semiquantitative PCR and quantitative PCR were performed as previously described.[22] The primers used for RT-PCR are listed in Table S2.

3 | RESULTS

3.1 | Gene expression profiles of wild-type and *ets1* mutant embryos revealed by RNA-Seq analysis

To further study the function of Ets1 during the NC development, we generated *X. tropicalis* mutant harboring mosaic mutations of *ets1* (G0 generation) using TALEN-mediated gene disruption (Figure 1A).[15] The G0 frog was then crossed with wild-type frog, and the offspring was raised to tadpole stage when genotyping was performed. An *ets1* mutant line with 13-bp deletion in the third exon was identified (Figure 1B). This mutation introduces a premature stop codon to the *ets1* open reading frame, leading to a truncated form of Ets1 without the majorities of protein domains, for example, TAD, Exon VII, and ETS domains (Figure 1B). After raised to adult, two heterozygous *ets1* mutant frogs were crossed to obtain the homozygous *ets1*$^{-/-}$ embryos. When the offspring developed to stage 17, a small posterior portion of the embryo where *ets1* expression is very low was dissected for genotyping (Figure 1C). Genotyping for individual embryos was performed with PCR using allele-specific primers and the mutation was then confirmed by sequencing (Figure 1D).

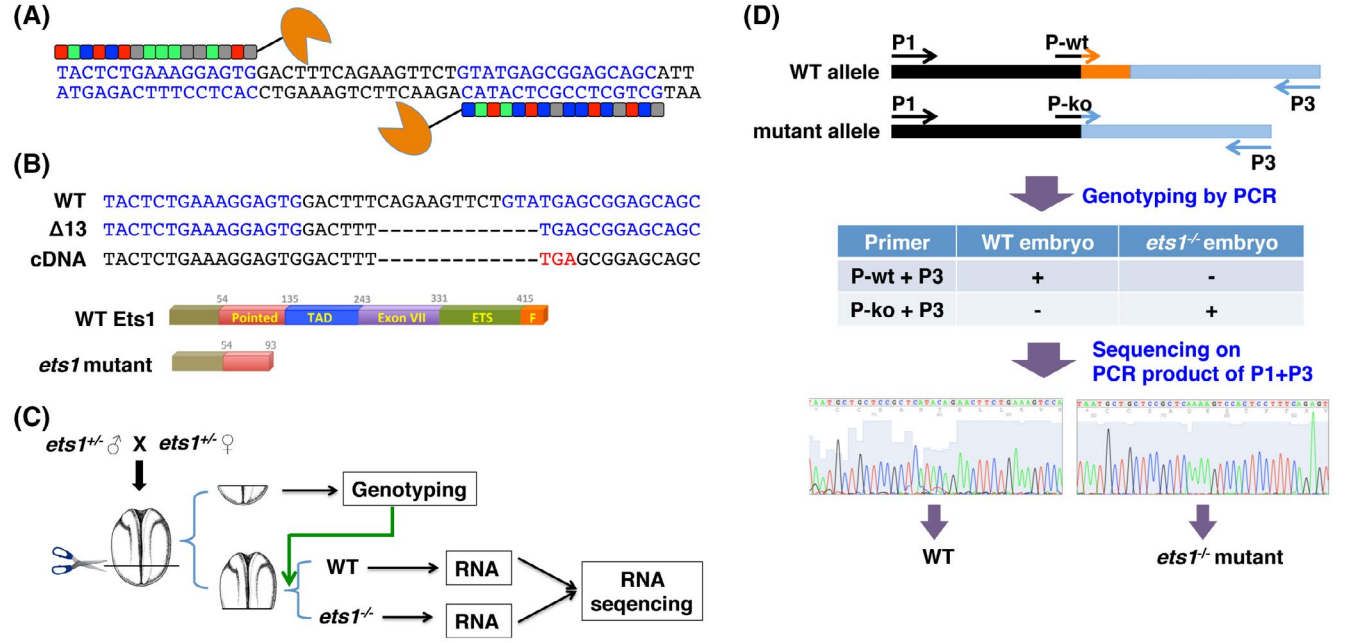

FIGURE 1 RNA sequencing on wild-type (WT) and *ets1* mutant embryos. A, TALENs were used to generate *ets1* mutant *X. tropicalis* frogs. The binding regions for TALEN-ets1 were marked in blue. B, Genotype of the *ets1* mutant line harboring mutant allele with 13-bp deletion. The complementary DNA (cDNA) that was reverse transcribed from RNA of *ets1* mutant embryos confirmed the 13-bp deletion, which generates a premature stop codon (marked by red). A truncated form of Ets1 with 93 amino acids was encoded in this *ets1* mutant. C, A schematic diagram showing the preparation of RNA samples used in RNA sequencing. D, Allele specific PCR was used for genotyping. P-wt primer can only bind to wild-type allele, while P-ko primer can specifically bind to *ets1* mutant allele. The genotyping result was further confirmed by sequencing on the PCR products.

The remaining parts of wild-type, heterozygous ($ets^{+/-}$) and homozygous *ets1* ($ets1^{-/-}$) mutant embryos were pooled for RNA extraction, respectively (Figure 1C; 15 embryos for each genotype). To confirm whether the 13-bp deletion also existed at the mRNA level, we amplified the 13-bp deletion *ets1* from $ets1^{-/-}$ mutant with RT-PCR and subcloned the amplicons into T-vector. Sequencing on five clones confirmed that all of them contained the 13-bp deletion (Figure 1B). Then, two batches of RNA samples prepared separately from wild-type and $ets1^{-/-}$ embryos were employed for RNA sequencing.

The RNA-Seq data were aligned to the version 9.1 *X. tropicalis* genome,[16] and gene expression was quantified as Reads Per Kilobase Million (RPKM). After comparing differently expressed genes between wild-type and $ets1^{-/-}$ embryos, the genes with both fold change greater than or equal to 2 and *P* value less than 0.05 were selected as differentially expressed genes (DEGs), which contains 169 transcripts (Table S1).

3.2 | Biological process annotation of the DEGs in *ets1* mutant embryos

To further delineate the functions of the selected 169 transcripts that are differentially expressed in *ets1* mutant embryos, we searched their gene symbols in NCBI database (https://www.ncbi.nlm.nih.gov/gene/) and GeneCards (www.genecards.org). Apart from 27 ncRNAs and 23 uncharacterized transcripts without any available annotation information, the remaining 119 transcripts were categorized based on their molecular functions, including transporter and ion channel (20%), enzyme (20%), protein, and other binding (13%), membrane receptor (10%), transcription factor (6%), ligand (3%), cytoskeletal proteins (3%), and uncategorized that cannot be assigned to the named groups (25%) (Figure 2A). Considering the diverse functions of the enzymes, they were further classified according to the types of reaction catalyzed. For the 24 enzymes in the list, about half of them (46%) were involved in the metabolic pathways (Figure 2B). The others were identified as protease and peptidase (21%), kinase (13%), phosphatase (8%), ubiquitin ligase (8%), and nuclease (4%) (Figure 2B).

Gene ontology analysis revealed important biological processes, in which the DEGs are involved (Figure 2C). It includes regulation of erythrocyte differentiation, regulation of vasodilation and blood circulation, which are related to the roles of Ets1 in hematopoiesis, vasculogenesis, and angiogenesis.[2] Some DEGs are involved in differentiation of pigment cell and melanocyte, such as *edn3* that has been reported to play an indispensable role in regulating melanocyte development.[23,24] In our RNA-Seq analysis, *edn3* was significantly reduced in $ets1^{-/-}$ mutant with

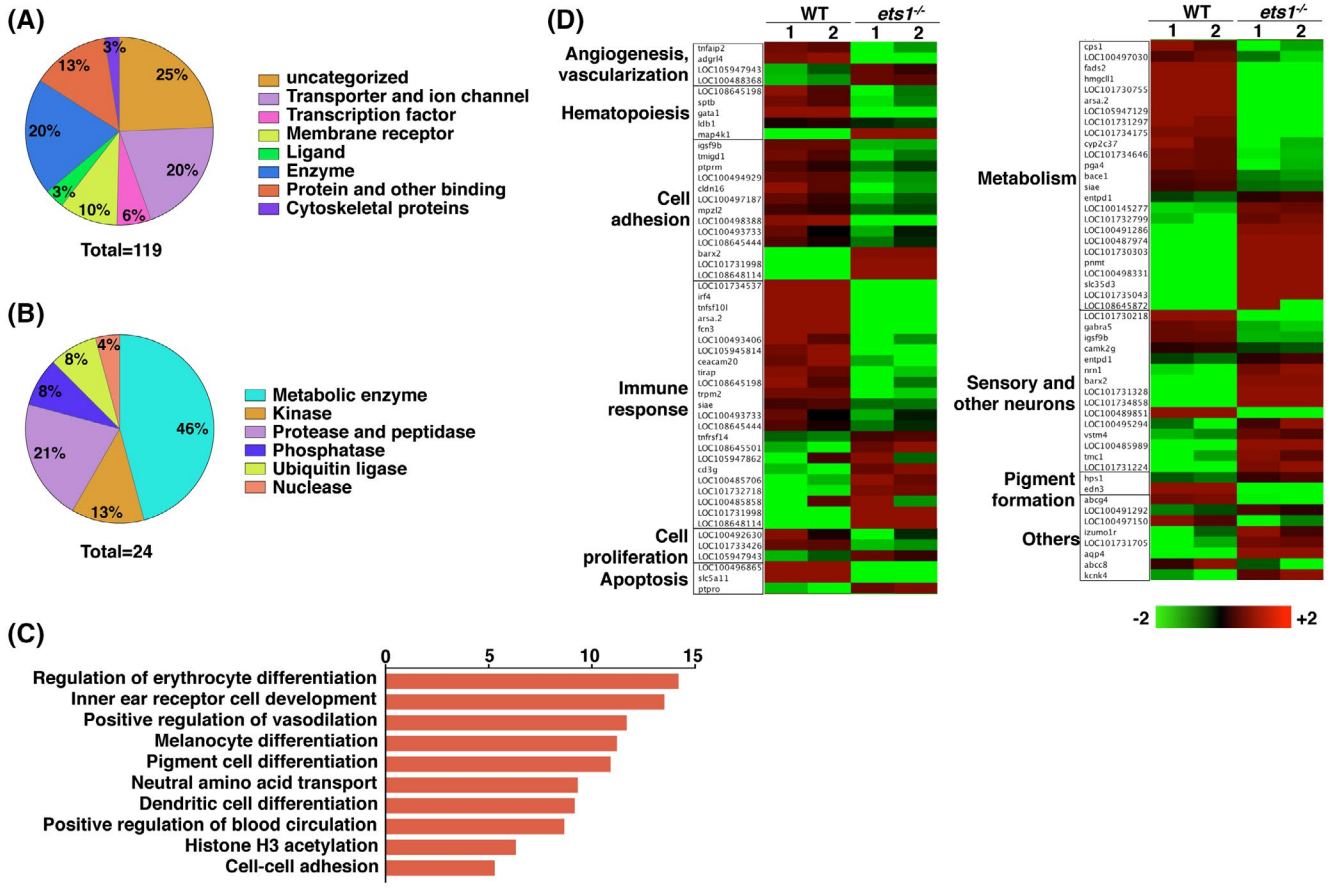

FIGURE 2 Biological process and heatmap analysis of the affected genes in *ets1* mutant. A, Total 119 genes up- or downregulated in *ets1* mutant were categorized according to their molecular functions. B, Twenty-four genes with enzymatic activity were grouped based on the reactions they catalyze. C, Gene Ontology analysis on the gene list revealed the biological processes they are involved in. D, Heatmap analysis on the 119 genes and they were also grouped according to their reported roles. The fold changes were taken logarithm with base 2, and the results were shown as a gradient from green (downregulated) to red (upregulated) over black (unchanged).

a 32-fold change relative to the WT embryos (Table S1), which may account for the pigment loss after knockdown of *ets1* in *Xenopus* embryos.[3] Regulation of histone H3 acetylation by the DEGs may be related to the interaction between Ets1 and epigenetic modulators, like Hdac1.[3,25] We also showed a heatmap with categorized genes based on their reported functions in GeneCards. The top two categories are immune response and metabolism, containing 23 genes and 25 genes, respectively. This finding implies the important roles of Ets1 in the two biological processes (Figure 2D). Moreover, four out of five genes involved in the hematopoiesis were downregulated in *ets1* mutant, such as *sptb*[26,27] and *gata1*,[28] suggesting a positively regulatory role of Ets1 in hematopoiesis-related genes (Figure 2D). Our data also suggest that Ets1 can regulate cell adhesion as 13 genes related with cell adhesion were identified in the DEGs, with 10 genes increased in *ets1* mutant. This observation suggests an implication of Ets1 in EMT and cell migration (Figure 2D). In contrast, 10 out of 15 genes related to sensory and other neurons were upregulated in *ets1* mutant (Figure 2D). Taken together, the gene ontology analysis revealed that Ets1 is involved in many biological processes in embryonic development.

3.3 | Validation of RNA-Seq analysis through quantitative RT-PCR

To validate the results of RNA-Seq, we examined the expression of 11 DEGs in WT, *ets1*$^{+/-}$ and *ets1*$^{-/-}$ embryos by quantitative RT-PCR (qPCR). A gene named *microseminoprotein beta gene 3* (*msmb3*), a member of the immunoglobulin binding factor family, showed reduced expression in *ets1*$^{+/-}$ and *ets1*$^{-/-}$ embryos in a dose-dependent manner (Figure 3A). Likewise, *tirap*, encoding a transmembrane receptor, was severely inhibited in *ets1*$^{-/-}$ embryos (Figure 3B). The expression of *igsf9b* that also encodes a transmembrane protein was reduced about 25% in *ets1*$^{-/-}$ mutant (Figure 3C). The expression level of *ncRNA435*, a noncoding RNA, in *ets1*$^{-/-}$ mutant was about half of that in WT embryos (Figure 3D). The expression of these four genes was also reduced in RNA-Seq analysis, with that of *tirap* decreased most severely (Table 1).

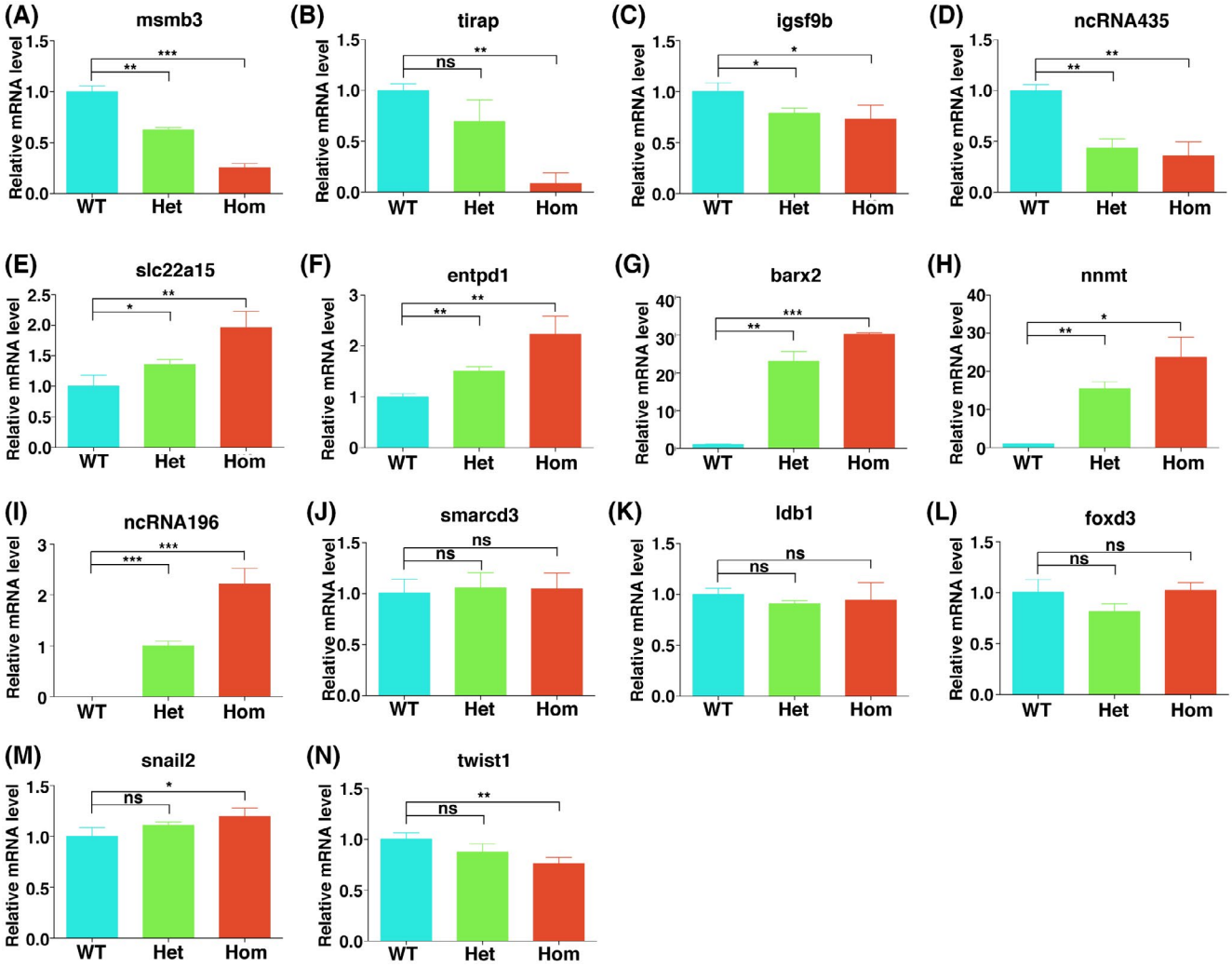

FIGURE 3 Quantitative RT-PCR analysis on the expression of selected genes in wild-type, heterozygous, and homozygous *ets1* mutant embryos of stage 17. A-D, The expression of *msmb3*, *tirap*, *igsf9b,* and *ncRNA435* was reduced in *ets1* mutant. E-I, The genes including *slc22a15*, *entpd1*, *barx2*, *nnmt,* and *ncRNA196* were activated in *ets1* mutant. J and K, The expression of *smarcd3* and *ldb1*, two genes with fold change less than two, was not obviously alternated in *ets1* mutant. L-N, The NC marker genes, *foxd3, snail2,* and *twist1*, were not affected obviously in *ets1* mutant. *Ornithine decarboxylase* (*odc*) was used as the internal control. WT, wild-type embryos; Het, heterozygous *ets1* mutant; Hom, homozygous *ets1* mutant. Unpaired *t* test was used to determine whether the difference between wild-type and heterozygous or homozygous *ets1* mutant was statistically significant. $*P < .05$, $**P < .01$, $***P < .001$. ns means no significant difference

In contrast, the expression of *slc22a15* and *entpd1*, two DEGs with positive fold changes in RNA-Seq analysis, showed two-fold increase in *ets1*$^{-/-}$ (Figure 3E,F; Table 1). We also detected the expression of *barx2*, *nnmt,* and *ncRNA196*, three genes with more than 10-fold changes in RNA-Seq analysis (Table 1). As the results showed, their expression levels in *ets1*$^{-/-}$ mutant were elevated more than 20-folds compared with those in WT embryos (Figure 3G-I). For these nine genes, the changes of their expression in qPCR were consistent well with those in RNA-Seq analysis. Furthermore, the qPCR results also showed that the expression values of the tested gene in *ets1*$^{+/-}$ were between those in *ets1*$^{-/-}$ and in *ets1*$^{+/+}$ embryos, suggesting that the changes in their expression were caused by loss of *ets1* specifically. For *smarcd3* and *ldb1* with fold changes of −1.79 and −1.46 in RNA-Seq analysis, their expression levels were not changed much in qPCR analysis (Figure 3J,K; Table 1), which may be due to the small values of fold change in RNA-Seq. Taken together, for the nine genes with fold change over two, all of them showed the same change trend between qPCR and RNA-Seq analysis, suggesting that the DEGs identified from RNA-Seq analysis are highly reliable.

We previously found that knockdown of *ets1* did not affect the NC specification, but suppressed NC migration in *Xenopus* embryos.[3] In line with this, the NC specifier genes, *foxd3* and *snail2*, were not affected much in *ets1*$^{-/-}$ embryos with the *snail2* slightly enhanced (Figure 3L, M). The NC migration marker, *twist1*, was mildly inhibited in *ets1*$^{-/-}$ mutant (Figure 3N). These observations further support the reliability of our RNA-Seq result.

TABLE 1 Gene symbols and fold changes of DEGs (*ets1*$^{-/-}$ mutant vs WT)

Gene title (this study)	Gene symbol	RNA locus	Fold change	*P* value
ankrd65	LOC101730332	XM_004920799	−5.76	.000177646
barx2	barx2	XM_002934879.4	13.68	7.18255E−06
cpras1	LOC100491292	XM_004916300.3	2.03	.036449763
entpd1	entpd1	NM_001006795.1	1.80	.008288789
fgf6L	LOC105947943	XM_018095520.1	3.28	.021782861
glipr2	LOC100497187	XM_002940737.4	−2.90	.019435267
igsf9b	igsf9b	XM_004916008.3	−3.86	.000449444
ldb1	ldb1	NM_213678.1	−1.46	.046333092
msmb.3	msmb.3	XM_002935960.4	−2.67	.005340114
ncRNA196	LOC108648196	XR_001924951.1	10.69	.001270678
ncRNA435	LOC100490435	XR_208799.3	−3.05	.008866055
nnmt	LOC100491286	XM_004916099.3	12.13	4.45559E−15
p3h1	LOC101734646	XM_012967249.2	−5.20	.002065368
plet1	LOC100498388	XM_002942422.4	−34.21	4.59757E−13
ppm1h	ppm1h	NM_001017305	−2.70	.00600537
slc22a15	slc22a15.2	NM_001045714.1	3.70	.000101065
slc25a16	LOC101731297	XM_004920701.3	−27.34	3.66842E−07
slc43a1	slc43a1	NM_001199911	−6.08	1.34124E−08
smarcd3	smarcd3	XM_018090234.1	−1.79	.00204267
tbata	LOC101731705	XM_004920499	4.37	.001191578
tirap	tirap	NM_001044460.1	−6.47	.00032059
wdfy4	wdfy4	XM_012967196	−2.50	.013533523

3.4 | Spatial expression patterns of the DEGs in *ets1* mutant embryos during embryonic development

We next sought to select some DEGs to study their expression patterns to further validate the RNA-Seq data by in situ hybridization. We have used three criteria to identify the transcripts, that is, high level of expression based on the data of RNA-Seq, lack of reported spatial expression pattern in Xenbase (http://www.xenbase.org), and potential roles in important biological processes as annotated in GeneCards. Thirteen transcripts were selected from the DEGs to study their expression patterns in *Xenopus* embryos at neurula and tailbud stages with whole mount in situ hybridization (WMISH). During neurulation, the signals of *msmb3* were visualized in cranial and trunk NC at stage 19, accompanied with weak staining in embryonic surface (Figure 4A). Then, the enrichment of *msmb3* signals in NC was lost at stage 20, and weak signals can only be observed on the surface of embryos (Figure 4B,C). From stage 21, strong *msmb3* expression was detected throughout the embryonic surface (Figure 4D), which is maintained during the tailbud stages (Figure 4E). Expression of *glipr2, fgf6L,* and *cpras1* was first detected in the migrating cranial NC at the end of neurula stage, and then, was maintained in early tailbud stages (Figure 4F-K). For *slc25a16* and *wdfy4*, their expression in NC was not observed until stage 25 (Figure 4L,M). Weak signals in migratory NC were also observed for *p3h1* and *ppm1h* in embryos at stage 25 (Figure 4N,P). However, their expression in brain and spinal cord becomes more evident around stage 32 (Figure 4O,Q). Taken together, these eight transcripts, for example, *msmb3*, *cpras1*, *slc25a16*, *wdfy4*, *glipr2*, *fgf6L*, *p3h1*, and *ppm1h,* are expressed in migratory NC, which was not reported before except for *glipr2*. Glipr2 was reported in a previous study showing identification of novel NC signature transcripts.[29]

Apart from NC, we also identified some genes that were expressed in other regions of the embryo. Among them, *plet1* and *ankrd65* showed expression in pronephros (Figure 4R-U). Strong signals of *plet1* were detected in pronephric tubule and duct (Figure 4S), while *ankrd65* signals were detected in the nephrostomes (Figure 4U). Moreover, both *plet1* and *tbata* are expressed in ventral blood island (Figure 4R,W), where *ets1* expression was also detected.[3] While *ankrd65* signals were detected in the heart anlage at stage 25 (Figure 4T), *tbata* was found in ciliated cells, brain, and the end of spinal cord (Figure 4V,W), and *slc43a1*, an amino acid transporter, was detected in somites and notochord at later tailbud stage

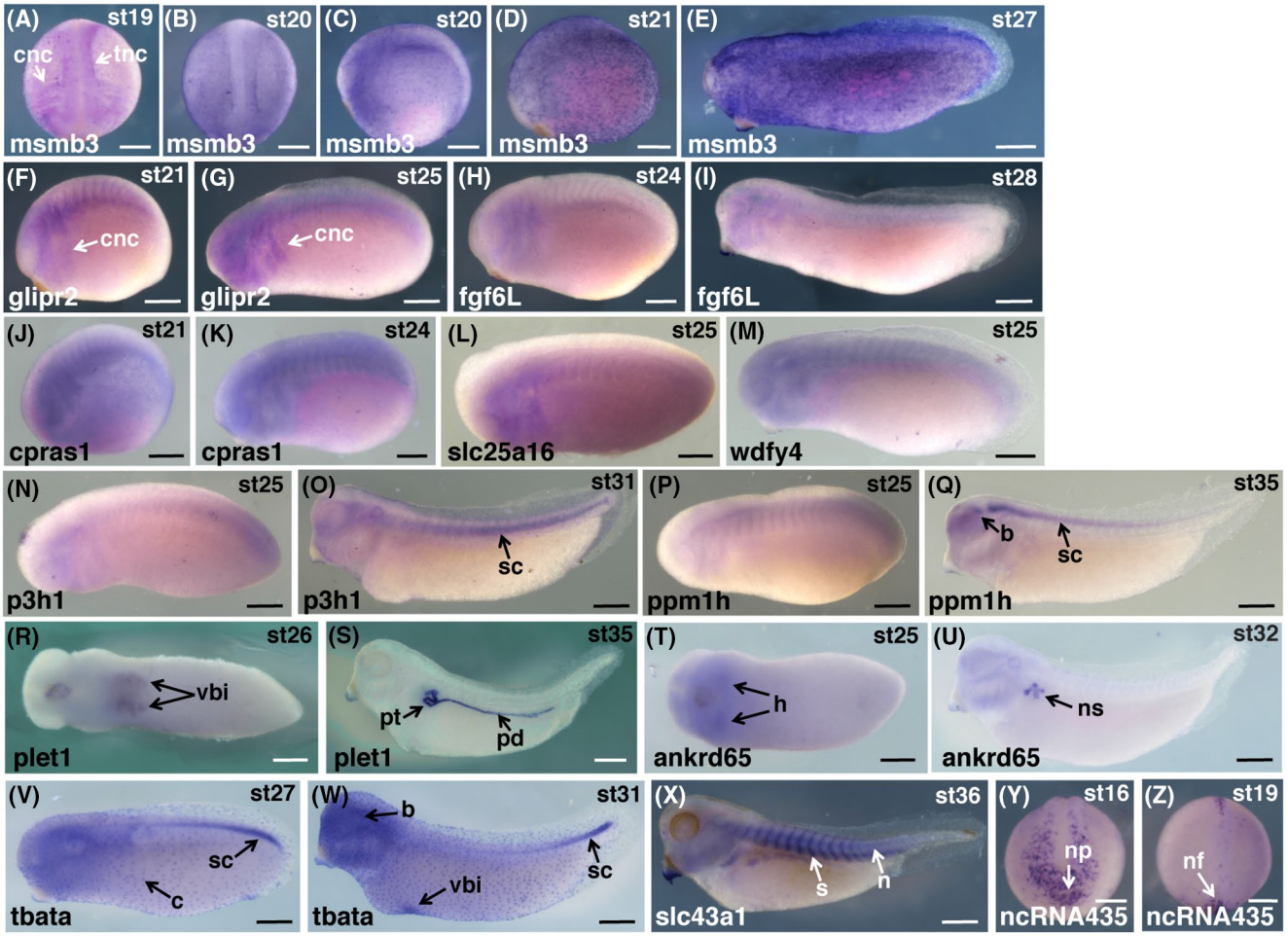

FIGURE 4 Whole mount in situ hybridization of the representative genes identified from RNA-Seq. The expression of a subset of affected genes in *ets1* mutant was analyzed in embryos at neurula or tailbud stage. A-E, The signals of *msmb3* were observed in migrating NC in late neurula stage (A), but then were enriched on surface of embryos (B-E). F-M, The expression of *glipr2*, *fgf6L*, *cpras1*, *slc25a16,* and *wdfy4* was detected in migrating NC during tailbud stages. N-Q, The expression of *p3h1* and *ppm1h* in migrating NC was observed at the beginning of tailbud stage, but then disappeared and changed to be evident in spinal cord. R-U, *plet1* and *ankrd65* were expressed in pronephros. *plet1* was detected in pronephric tubule and duct (S), and the *ankrd65* was detected in nephrostomes (U). Apart from the pronephros, *plet1* was also observed in ventral blood island (R), and *ankrd65* was expressed in heart anlage (T). V-Z, The expression of *tbata* was detected in cilia, ventral blood island, and the end of spinal cord (V, W), *slc43a1* was detected in somites, pronephros (X), and the *ncRNA435* expression was detected in anterior neural plate as signal dots (Y, Z). b, brain; c, ciliated cell; cnc, cranial neural crest cells; h, heart anlage; n, notochord; nf, neural fold; np, neural plate; ns, nephrostomes; pd, pronephric duct; pt, pronephric tubule; s, somite; sc, spinal cord; tnc, trunk neural crest; vbi, ventral blood island. Scale bar = 1000 μm

(Figure 4X). We also examined expression pattern of a non-coding RNA, *ncRNA435*, which showed spot like signals in neural fold and anterior region of the neural plate at stage 16 (Figure 4Y). This expression is the reminisce of *slc12a10.2*, *trpv5/6*, and *atp6v1a1* showing signal spots on epidermis.[30] The expression pattern of *ncRNA435* suggests a role of this gene in neural tube closure as only the signals in the neural fold were visible after neural tube closure (Figure 4Z). Taken together, the DEGs identified in *ets1*$^{-/-}$ mutant showed expression in migrating NC and other tissues of the embryo, suggesting diversity of their functions in NC migration and other developmental processes such as development of pronephros, ventral blood island, and heart.

3.5 | The expression of *msmb3* is positively regulated by Ets1

Since *msmb3* expression was detected in the migrating NC at later neurula stage, we further studied on the regulation of *msmb3* expression by Ets1. In line with the reduction of *msmb3* expression in *ets1*$^{-/-}$ embryos, overexpression of *ets1* mRNA strongly upregulated *msmb3* (Figure 5A). In *X. tropicalis*, there are another four members of the msmb family, including *msmb1* (XM_002935969), *msmb2* (XM_004915922), *msmb4* (XM_031905784), and *msmb5* (XM_002935961). We also examined whether their expression is regulated by *ets1* with qPCR. It turned out that the expression of either of

them was extremely low (Ct values > 35) in the control or *ets1* mRNA injected embryos at stage 17 (Figure 5A), indicating that *msmb3* is the dominant msmb form at this stage. The dependence of *msmb3* expression on Ets1 was further confirmed by WMISH, which showed reduction of *msmb3* upon knockdown of *ets1* with antisense morpholino oligonucleotides targeting *ets1* (ets1MO) (Figure 5B). Collectively, these results indicate that Ets1 is necessary and sufficient to induce *msmb3* expression in *X. tropicalis*. Two orthologs of *msmb3* were identified in *X. laevis*, *msmb3L* (Sequence in Supporting Information 1) and *msmb3S* (XM_018227125.1). The expression of *msmb3S* was not detected in any of the examined stages through RT-PCR (Figure S1). We then focused on studying *msmb3L* in *X. laevis*. The expression of *msmb3L* was barely detected at early neurula stage, but weak signals appeared from stage 18 when NC emigration begins (Figure S1). Its expression was gradually increased during tailbud stages (Figure S1). *Xenopus* animal cap can be induced into NC tissue by overexpression of *wnt3a* and *chordin*, as revealed by the induction of *foxd3* expression, and

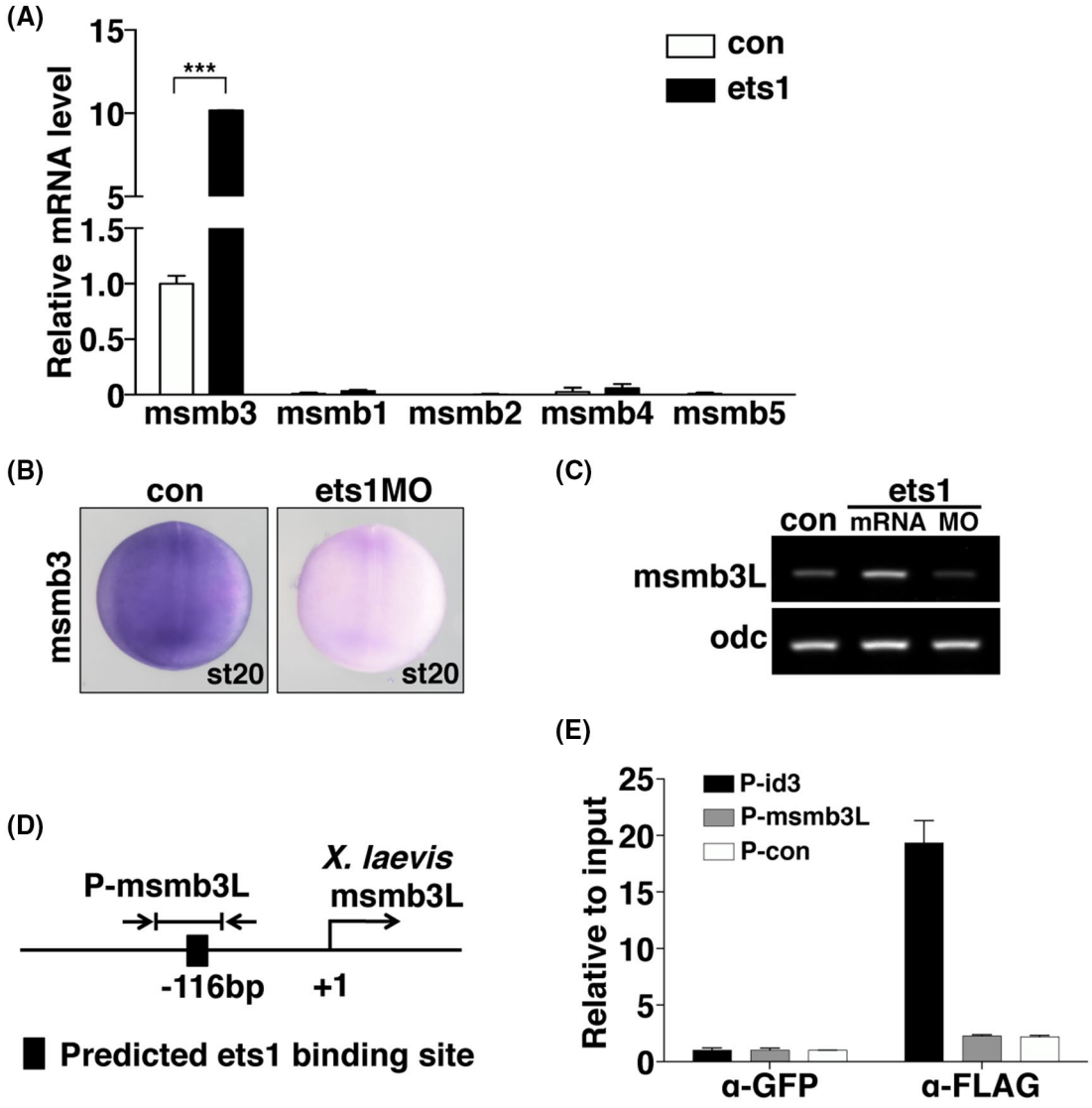

FIGURE 5 The expression *of msmb3* was positively regulated by Ets1. A, qPCR showed that *ets1* overexpression efficiently induced the expression of *msmb3*, but not the other msmb members including *msmb1*, *msmb2*, *msmb4,* and *msmb5*. ***$P < .001$ by t test. B, Whole mount in situ hybridization demonstrated the reduction of *msmb3* expression in *X. tropicalis* embryos injected with ets1MO (19 of 20 embryos). C, The expression of *msmb3L* was enhanced by *ets1* overexpression and repressed by knockdown of *ets1*. Either *ets1* mRNA or MO was injected into *X. laevis* embryos. The injected embryos were collected at stage 19 for RNA extraction. RT-PCR was used to examine the expression of *msmb3L*. D and E, ChIP was performed in *X. laevis* embryos injected with *ets1-FLAG* mRNA. The anti-FLAG and anti-GFP antibodies were used to precipitate the protein extracts. Quantitative PCR was done using primer pair P-msmb3L bridging the predicted Ets1 binding site in *msmb3L* promoter (D). Ets1 did not bind to the predicted site in the *msmb3L* promoter region. Primers targeting *id3* promoter (P-id3) was used as a positive control. P-con, negative control primer pair. Error bars represent standard deviation.

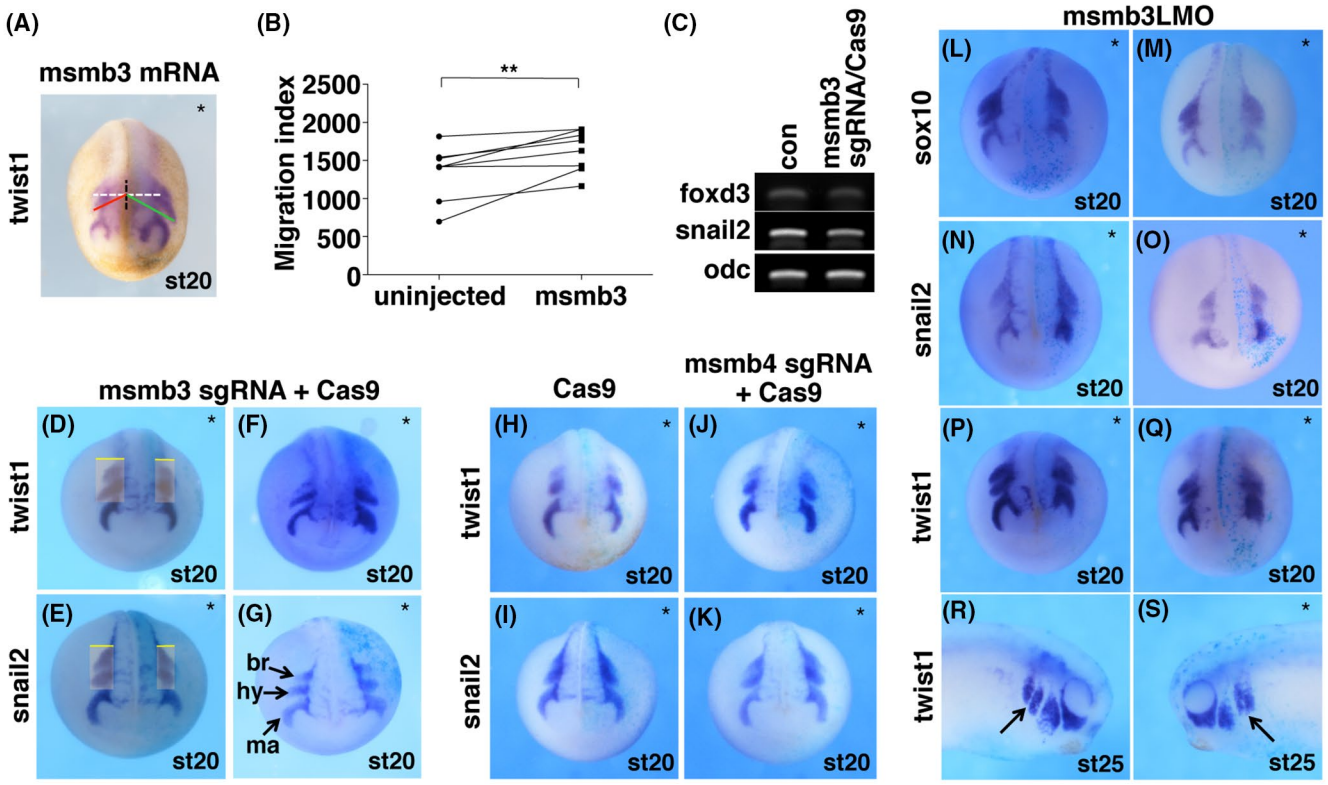

FIGURE 6 Msmb3 is required to maintain NC migration patterns in *Xenopus*. A, *msmb3* mRNA was co-injected with *lacZ* mRNA into one dorsal blastomere at 4-cell stage. After LacZ staining, whole mount in situ hybridization was performed using probe of *twist1*. The asterisk indicates the injected side. The NC migration index on control side and *msmb3* injected side is defined as the length of the red line and green line, respectively. The line was drawn from dorsal midline to the pioneer cell of hyoid stream. B, Eight embryos with LacZ staining covering the NC region were used to measure the migration index. A paired *t* test was used to compare the migration index between injected and uninjected side, and a significant change was detected. Double-asterisk represents *P* value < .01 by paired *t* test. C-G, NC migration, but not NC formation, was affected in *X. tropicalis* embryos after CRISPR/Cas9-mediated gene disruption at *msmb3* locus. The Cas9 protein and *msmb3* sgRNA were co-injected into embryos at one-cell stage. When the embryos developed to stage 20, total RNA was extracted for the analysis of NC marker expression with RT-PCR (C). The mixture of Cas9 protein, *msmb3* sgRNA, and *lacZ* mRNA was injected into one blastomere of two-cell stage embryos. The embryos were collected at stage 20 for LacZ staining. WMISH showed that NC migration streams labeled by *twist1* (50%, 9 of 18 embryos) and *snail2* (63%, 17 of 27 embryos) signals became shorter and thickened on the injected side (D-G). The migration distance of hyoid NC stream was demonstrated by yellow line (D, E). br, branchial crest; hy, hyoid crest; ma, mandibular crest. H-K, Single injection of Cas9 protein (H, 96%, 27 of 28 embryos; I, 100%, 27 of 27 embryos) or injection of CRISPR/Cas9 targeting *msmb4* (J, 100%, 24 of 24 embryos; K, 100%, 25 of 25 embryos) did not affect NC migration. L-S, The MO targeting *X. laevis msmb3L* (msmb3LMO) was co-injected with *lacZ* mRNA into one dorsal blastomere at four-cell stage. The injected embryos were collected at stage 20 (L-Q) or 25 (R, S) for LacZ staining, and then, WMISH was performed. Knockdown of *msmb3L* caused similar migration defects in NC markers of *sox10* (69.2%, 9 out of 13 embryos), *snail2* (62.5%, 10 out of 16 embryos), and *twist1* (65%, 13 out of 20 embryos at stage 20; 50%, 10 out of 20 embryos at stage 25). The asterisk indicates the injected side. The arrow in R, S showed that the boundary between brachial streams disappeared after msmb3LMO injection.

msmb3L expression was also upregulated along with *foxd3* (Figure S2). This is in line with the enrichment of *msmb3* in NC of *X. tropicalis* embryos (Figure 4A). Similar to *msmb3* in *X. tropicalis*, *msmb3L* expression in *X. laevis* was also promoted by overexpression of *ets1*, and inhibited by knockdown of *ets1* (Figure 5C). These results indicated that *msmb3* expression was positively regulated by Ets1 in both *X. laevis* and *X. tropicalis* embryos. However, chromatin immunoprecipitation failed to detect the binding of Ets1 to the predicted binding site in *msmb3L* promoter, suggesting Ets1 may use other mechanisms to regulate *msmb3L* expression (Figure 5D,E).

3.6 | Msmb3 is required for maintaining the NC migration pattern

To study the functions of Msmb3 in NC migration, we injected *msmb3* mRNA into one dorsal blastomere of *X. laevis* embryos at four cell stage. The *lacZ* mRNA was co-injected to trace the injected side. When developing to stage 20, the embryos were collected for WMISH using probe of *twist1*, which is a marker gene for NC migration. The migration of NC was evaluated by the distance between dorsal midline and distal end of hyoid NC stream, which is designated as the migration index (Figure 6A). Paired comparison between the *msmb3* injected

and the uninjected side showed that overexpression of *msmb3* promoted the NC migration index significantly (Figure 6B). Then, we used CRISPR/Cas9 to disrupt the endogenous *msmb3* gene. The sgRNA targeting *X. tropicalis msmb3* was designed and co-injected with Cas9 protein into one-cell stage embryos (Figure 6C-K), and the injection with the Cas9 protein alone was served as the negative control (Figure 6H,I). T7E1 assay revealed that the disruption efficiency was 29% (Figure S3A). The expression levels of NC marker genes, *foxd3* and *snail2*, were only mildly decreased in the injected embryos as shown by RT-PCR (Figure 6C). Next, the Cas9 protein, *msmb3* sgRNA, and *lacZ* mRNA were co-injected into one blastomere of two-cell stage embryos, and then, WMISH was performed to assess expression of *twist1* and *snail2* in the injected embryos. Compared with the uninjected side, the migration distance of NC stream was shorter in the injected side at late neurula stage (Figure 6D-G). These defects were more evident in the hyoid and branchial crest, as shown by the signals of *twist1* and *snail2* (Figure 6D,E). In some embryos, the migration distance of hyoid and branchial crest was not reduced. However, the NC migration streams, especially the mandibular crest, became thicker and cannot migrate further toward the ventral side at the injected side (Figure 6F,G). We have also performed the microinjection with the sgRNAs targeting *msmb4*, another member of the msmb family in *X. tropicalis*. Like the injection with Cas9 protein alone (Figure 6H,I), co-injection of Cas9 protein and *msmb4* sgRNA (Figure 6J,K) did not cause defects in NC migration stream, although 52% gene disruption efficiency was induced by *msmb4* sgRNA (Figure S3B). We also designed a MO targeting *X. laevis msmb3L* (msmb3LMO) since *msmb3S* transcripts were not detected (Figure S1). After injection of msmb3LMO in one dorsal blastomere of four-cell stage embryos, WMISH was performed to visualize migrating NC with the probes of *sox10*, *snail2*, and *twist1* (Figure 6L-S). Knockdown of *msmb3L* disrupted the NC migration pattern, which is similar to the phenotypes observed in *X. tropicalis* embryos. The mandibular crest was thickened and cannot extend laterally as far as those at the uninjected side (Figure 6L-Q). The space between hyoid and branchial crest disappeared, and the two NC streams were fused together (Figure 6L-Q). At the tailbud stages, the anterior and posterior branchial crest cannot be separated completely at the msmb3LMO-injected side (Figure 6R,S). These findings suggest that Msmb3 is involved in the separation of different NC streams and patterning of NC migration.

4 | DISCUSSION

In this study, we performed RNA-Seq analysis on the embryos of wild-type and *ets1* mutant *X. tropicalis*, through which we identified Ets1 downstream genes during early embryonic development. We then selected some genes for examining their spatial expression patterns. Several genes were expressed in migrating NC, including *msmb3*, *cpras1*, *slc25a16*, *wdfy4*, *glipr2*, *fgf6l*, *p3h1*, and *ppm1h* (Figure 4A-Q). The studies about their functions in cell migration are limited. Overexpression of *GLIPR2* has been reported to promote EMT and migration in HK-2 cells, and may be responsible for renal fibrosis.[31] WDFY4 is predominately expressed in primary and secondary immune tissues with unknown function.[32] Both ETS1 and WDFY4 are closely related with systemic lupus erythematosus,[32] suggesting their involvement in immune system. The expression of *plet1* and *tbata* in ventral blood island, and *ankrd65* in heart anlage (Figure 4R-W) is in line with the roles of Ets1 in regulating blood formation and heart development.[7,11,33] *plet1* and *ankrd65* signals were also detected in the pronephros (Figure 4R-U), which were downregulated in embryo after knockdown of *ets1* (data not shown). Whether Ets1 functions in regulating pronephros formation needs to be further studied. *nectin2*, another Ets1 downstream gene we identified (LOC108645444 in Table S1), has been reported to regulate neural tube morphogenesis in *Xenopus*.[34] It was expressed in neural fold during neurulation and knockdown of *nectin2* impaired neural fold formation. Nectin2 cooperates with N-cadherin to enhance apical constriction via driving accumulation of F-actin at the apical cell surface.[34] Interestingly, we identified a noncoding RNA, *ncRNA435*, shared similar expression pattern with *nectin2*. It showed expression in the neural fold surrounding the median hinge during neurulation (Figure 4Y). After neural folds closure, the signals were almost not detected on surface, only leaving some signal spots in the midline (Figure 4Z). The expression pattern of *ncRNA435* corresponds to a possible role in neural tube closure. Collectively, the diversity of expression patterns of the Ets1 target genes suggests that Ets1 regulates a large range of developmental processes.

We focus on studying msmb3, a novel transcript upregulated by *ets1* identified in this analysis. In human, MSMB is synthesized by the epithelial cells of the prostate gland and is one of three predominant proteins secreted to prostatic fluid.[35] Consistent with this, the secretion of Myc-tagged Msmb3 is confirmed in HEK293T cells (data not shown). Although several studies have suggested that MSMB plays a tumor suppressive role in human prostate cancer,[36-40] emerging evidence show that elevated MSMB expression level was observed in ovarian cancer cell lines and patients,[41] and that increased intratumoral expression of MSMB was suggested to be associated with unfavorable disease outcomes.[42] Since upregulation of *ETS1* was found in prostate carcinoma glands[43] and high ETS1 expression is associated with poor tumor differentiation,[44] whether the Ets1/Msmb3 axis is involved in tumorigenesis of these cancers is an important question worth further investigation. Interestingly, although *msmb3* expression is regulated by Ets1, Ets1 does not seem to bind to the proximal promoter of *Xenopus msmb3L* (Figure 5D,E). It has been reported that Ets1 regulates *Sox10* and *Gata4* in chick and mouse through binding to the *cis*-regulatory elements,

such as enhancers, in a tissue-specific manner.[9,45-47] We speculated that Ets1 may regulate *msmb3* expression in a similar way, which await further study.

NC is a transient cell population, which is highly migratory. Indeed, the NC cells are guided and migrate along the specific routes that are defined by the interaction with molecules in the extracellular matrix and by communication with the membrane proteins of adjacent cells. Failure of NC migration causes numerous human diseases such as Waardenburg-Shah syndrome (WS4A)[48] and Hirschsprung disease.[49] *TBX1*, the leading gene candidate for DiGeorge (DGS) and velocardiofacial syndrome (VCFS), was found to affect cardiac NC cells migration through altering its surrounding microenvironment.[50,51] Ets1 is required for proper migration and differentiation of NC. The expression of *msmb3*, but not other *msmb* members, was positively regulated by Ets1 in *Xenopus* embryos (Figures 3A and 5A-C). Consistent with this notion, we demonstrate that Msmb3 is involved in patterning NC migration by preventing NC streams from fusing. Similar effects of secreted proteins on NC migration have been reported previously.[52] Two secreted Semaphorins, Sema 3A and Sema 3F, which are expressed and secreted within the neural crest-free mesenchyme of chicken hindbrain, contributes to the restriction and maintenance of NC cell streams through interaction with Neuropilin, their receptors expressed in NC.[52] Thus, it is possible that Msmb3 is secreted by migratory NC cells and helps to maintain the boundary of NC streams through interaction with its receptors expressed in adjacent non-NC cells. Clearly, future studies are required to further elucidate the function of Msmb3 in NC migration.

ACKNOWLEDGMENTS

This work is supported by National Key R&D Program of China, Grant/Award Number: 2016YFE0204700, the Research Grants Council of Hong Kong (14167017, and 14112618) to HZ, and the International Partnership Program of Chinese Academy of Sciences (152453KYSB20170031) to YGY and HZ. Additional support was provided by Hong Kong Branch of CAS Center for Excellence in Animal Evolution and Genetics, The Chinese University of Hong Kong.

CONFLICTS OF INTEREST

The authors decare that there is no conflict of interest regarding the contents of this article.

AUTHOR CONTRIBUTIONS

C. WANG and H. Zhao designed research; C. Wang performed experiments; X. Zhou, X. Chen, and Z. Jiang analyzed the raw RNA-Seq data; C. Wang, X. Qi, J. Sun, D. Cai, G. Lu, and H. Zhao analyzed and interpreted the results; C. WANG and H. Zhao wrote the paper; Y. Yao and W.Y. Chan provided analytical tools for this study.

REFERENCES

1. Nye JA, Petersen JM, Gunther CV, Jonsen MD, Graves BJ. Interaction of murine ets-1 with GGA-binding sites establishes the ETS domain as a new DNA-binding motif. *Genes Dev*. 1992;6:975-990.
2. Dittmer J. The biology of the Ets1 proto-oncogene. *Mol Cancer*. 2003;2:29.
3. Wang C, Kam RK, Shi W, et al. The proto-oncogene transcription factor Ets1 regulates neural crest development through histone deacetylase 1 to mediate output of bone morphogenetic protein signaling. *J Biol Chem*. 2015;290:21925-21938.
4. Dittmer J. The role of the transcription factor Ets1 in carcinoma. *Semin Cancer Biol*. 2015;35:20-38.
5. Tahtakran SA, Selleck MA. Ets-1 expression is associated with cranial neural crest migration and vasculogenesis in the chick embryo. *Gene Expr Patterns*. 2003;3:455-458.
6. Theveneau E, Duband JL, Altabef M. Ets-1 confers cranial features on neural crest delamination. *PLoS One*. 2007;2:e1142.
7. Gao Z, Kim GH, Mackinnon AC, et al. Ets1 is required for proper migration and differentiation of the cardiac neural crest. *Development*. 2010;137:1543-1551.
8. Nie S, Bronner ME. Dual developmental role of transcriptional regulator Ets1 in Xenopus cardiac neural crest vs. heart mesoderm. *Cardiovasc Res*. 2015;106:67-75.
9. Schachterle W, Rojas A, Xu SM, Black BL. ETS-dependent regulation of a distal Gata4 cardiac enhancer. *Dev Biol*. 2012;361:439-449.
10. Wei G, Srinivasan R, Cantemir-Stone CZ, et al. Ets1 and Ets2 are required for endothelial cell survival during embryonic angiogenesis. *Blood*. 2009;114:1123-1130.
11. Marziali G, Perrotti E, Ilari R, et al. Role of Ets-1 in erythroid differentiation. *Blood Cells Mol Dis*. 2002;29:553-561.
12. Seth A, Robinson L, Thompson DM, Watson DK, Papas TS. Transactivation of GATA-1 promoter with ETS1, ETS2 and ERGB/Hu-FLI-1 proteins: stabilization of the ETS1 protein binding on GATA-1 promoter sequences by monoclonal antibody. *Oncogene*. 1993;8:1783-1790.
13. Russell L, Garrett-Sinha LA. Transcription factor Ets-1 in cytokine and chemokine gene regulation. *Cytokine*. 2010;51:217-226.
14. Garrett-Sinha LA. Review of Ets1 structure, function, and roles in immunity. *Cell Mol Life Sci*. 2013;70:3375-3390.
15. Lei Y, Guo X, Liu Y, et al. Efficient targeted gene disruption in Xenopus embryos using engineered transcription activator-like effector nucleases (TALENs). *Proc Nat Acad Sci*. 2012;109(43):17484-17489
16. Hellsten U, Harland RM, Gilchrist MJ, et al. The genome of the Western clawed frog Xenopus tropicalis. *Science*. 2010;328:633-636.
17. Robinson MD, McCarthy DJ, Smyth GK. edgeR: a Bioconductor package for differential expression analysis of digital gene expression data. *Bioinformatics*. 2010;26:139-140.
18. Shi W, Xu G, Wang C, et al. Heat shock 70-kDa protein 5 (Hspa5) is essential for pronephros formation by mediating retinoic acid signaling. *J Biol Chem*. 2015;290:577-589.
19. Nieuwkoop PD,Faber J. *Normal Table of* Xenopus laevis *(Daudin): A Systematicsal and Chronological Survey of the Development Form the Fertilized Egg Till the End of Metamorphosis*. New York: Garland Pub.; 1994.
20. Harland RM. In situ hybridization: an improved whole-mount method for *Xenopus embryos*. *Methods Cell Biol*. 1991;36:685-695.
21. Akkers RC, Jacobi UG, Veenstra GJ. Chromatin immunoprecipitation analysis of *Xenopus embryos*. *Methods Mol Biol*. 2012;917:279-292.

22. Wang CD, Guo XF, Wong TCB, et al. Developmental expression of three prmt genes in *Xenopus*. *Zool Res*. 2019;40:102-107.
23. Aoki H, Motohashi T, Yoshimura N, et al. Cooperative and indispensable roles of endothelin 3 and KIT signalings in melanocyte development. *Dev Dynam*. 2005;233:407-417.
24. Hou L, Pavan WJ, Shin MK, Arnheiter H. Cell-autonomous and cell non-autonomous signaling through endothelin receptor B during melanocyte development. *Development*. 2004;131:3239-3247.
25. Lee CG, Kwon HK, Sahoo A, et al. Interaction of Ets-1 with HDAC1 represses IL-10 expression in Th1 cells. *J Immunol*. 2012;188:2244-2253.
26. Bloom ML, Kaysser TM, Birkenmeier CS, Barker JE. The murine mutation jaundiced is caused by replacement of an arginine with a stop codon in the mRNA encoding the ninth repeat of beta-spectrin. *Proc Natl Acad Sci USA*. 1994;91:10099-10103.
27. Liao EC, Paw BH, Peters LL, et al. Hereditary spherocytosis in zebrafish riesling illustrates evolution of erythroid beta-spectrin structure, and function in red cell morphogenesis and membrane stability. *Development*. 2000;127:5123-5132.
28. Ferreira R, Ohneda K, Yamamoto M, Philipsen S. GATA1 function, a paradigm for transcription factors in hematopoiesis. *Mol Cell Biol*. 2005;25:1215-1227.
29. Plouhinec JL, Roche DD, Pegoraro C, et al. Pax3 and Zic1 trigger the early neural crest gene regulatory network by the direct activation of multiple key neural crest specifiers. *Dev Biol*. 2014;386:461-472.
30. Dai W, Bai Y, Hebda L, et al. Calcium deficiency-induced and TRP channel-regulated IGF1R-PI3K-Akt signaling regulates abnormal epithelial cell proliferation. *Cell Death Differ*. 2014;21:568-581.
31. Huang S, Liu F, Niu Q, et al. GLIPR-2 overexpression in HK-2 cells promotes cell EMT and migration through ERK1/2 activation. *PLoS One*. 2013;8:e58574.
32. Yang W, Shen N, Ye DQ, et al. Genome-wide association study in Asian populations identifies variants in ETS1 and WDFY4 associated with systemic lupus erythematosus. *PLoS Genet*. 2010;6:e1000841.
33. Marziali G, Perrotti E, Ilari R, et al. Role of Ets-1 in transcriptional regulation of transferrin receptor and erythroid differentiation. *Oncogene*. 2002;21:7933-7944.
34. Morita H, Nandadasa S, Yamamoto TS, Terasaka-Iioka C, Wylie C, Ueno N. Nectin-2 and N-cadherin interact through extracellular domains and induce apical accumulation of F-actin in apical constriction of *Xenopus* neural tube morphogenesis. *Development*. 2010;137:1315-1325.
35. Lilja H, Abrahamsson PA. Three predominant proteins secreted by the human prostate gland. *Prostate*. 1988;12:29-38.
36. Bjartell AS, Al-Ahmadie H, Serio AM, et al. Association of cysteine-rich secretory protein 3 and beta-microseminoprotein with outcome after radical prostatectomy. *Clin Cancer Res*. 2007;13:4130-4138.
37. Garde SV, Basrur VS, Li L, et al. Prostate secretory protein (PSP94) suppresses the growth of androgen-independent prostate cancer cell line (PC3) and xenografts by inducing apoptosis. *Prostate*. 1999;38:118-125.
38. Hyakutake H, Sakai H, Yogi Y, et al. Beta-microseminoprotein immunoreactivity as a new prognostic indicator of prostatic carcinoma. *Prostate*. 1993;22:347-355.
39. Liu AY, Bradner RC, Vessella RL. Decreased expression of prostatic secretory protein PSP94 in prostate cancer. *Cancer Lett*. 1993;74:91-99.
40. Nam RK, Reeves JR, Toi A, et al. A novel serum marker, total prostate secretory protein of 94 amino acids, improves prostate cancer detection and helps identify high grade cancers at diagnosis. *J Urology*. 2006;175:1291-1297.
41. Ma JX, Yan BX, Zhang J, et al. PSP94, an upstream signaling mediator of prostasin found highly elevated in ovarian cancer. *Cell Death Dis*. 2014;5:e1407.
42. Girvan AR, Chang P, van Huizen I, et al. Increased intratumoral expression of prostate secretory protein of 94 amino acids predicts for worse disease recurrence and progression after radical prostatectomy in patients with prostate cancer. *Urology*. 2005;65:719-723.
43. Shaikhibrahim Z, Langer B, Lindstrot A, et al. Ets-1 is implicated in the regulation of androgen co-regulator FHL2 and reveals specificity for migration, but not invasion, of PC3 prostate cancer cells. *Oncol Rep*. 2011;25:1125-1129.
44. Alipov G, Nakayama T, Ito M, et al. Overexpression of Ets-1 proto-oncogene in latent and clinical prostatic carcinomas. *Histopathology*. 2005;46:202-208.
45. Betancur P, Bronner-Fraser M, Sauka-Spengler T. Genomic code for Sox10 activation reveals a key regulatory enhancer for cranial neural crest. *Proc Natl Acad Sci USA*. 2010;107:3570-3575.
46. Betancur P, Sauka-Spengler T, Bronner M. A Sox10 enhancer element common to the otic placode and neural crest is activated by tissue-specific paralogs. *Development*. 2011;138:3689-3698.
47. Saldana-Caboverde A, Perera EM, Watkins-Chow DE, et al. The transcription factors Ets1 and Sox10 interact during murine melanocyte development. *Dev Biol*. 2015;407:300-312.
48. Edery P, Attie T, Amiel J, et al. Mutation of the endothelin-3 gene in the Waardenburg-Hirschsprung disease (Shah-Waardenburg syndrome). *Nat Genet*. 1996;12:442-444.
49. Tobin JL, Di Franco M, Eichers E, et al. Inhibition of neural crest migration underlies craniofacial dysmorphology and Hirschsprung's disease in Bardet-Biedl syndrome. *Proc Natl Acad Sci U S A*. 2008;105:6714-6719.
50. Calmont A, Ivins S, Van Bueren KL, et al. Tbx1 controls cardiac neural crest cell migration during arch artery development by regulating Gbx2 expression in the pharyngeal ectoderm. *Development*. 2009;136:3173-3183.
51. Vitelli F, Morishima M, Taddei I, Lindsay EA, Baldini A. Tbx1 mutation causes multiple cardiovascular defects and disrupts neural crest and cranial nerve migratory pathways. *Hum Mol Genet*. 2002;11:915-922.
52. Osborne NJ, Begbie J, Chilton JK, Schmidt H, Eickholt BJ. Semaphorin/neuropilin signaling influences the positioning of migratory neural crest cells within the hindbrain region of the chick. *Dev Dynam*. 2005;232:939-949.

SUPPORTING INFORMATION

Additional supporting information may be found online in the Supporting Information section.

How to cite this article: Wang C, Qi X, Zhou X, et al. RNA-Seq analysis on *ets1* mutant embryos of *Xenopus tropicalis* identifies *microseminoprotein beta gene 3* as an essential regulator of neural crest migration. *The FASEB Journal*. 2020;34:12726–12738. https://doi.org/10.1096/fj.202000603R

Supplementary Data

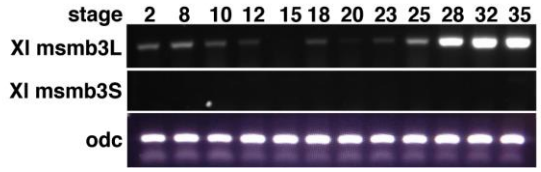

Supplementary Figure 1. The expression of *msmb3L*, but not *msmb3S*, was detected in *X. laevis* embryos. RT-PCR was performed to examine the expression of *msmb3L* and *msmb3S* in *X. laevis* embryos at different stages. *odc* was used as loading control.

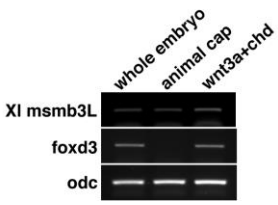

Supplementary Figure 2. The expression of *msmb3L* was up-regulated by co-expression of *wnt3a* and *chordin* in animal cap assay. The mixture of *wnt3a* and *chordin* mRNAs was co-injected into the animal pole of two cell stage *X. laevis* embryos. Animal caps were dissected at stage 9 and cultured until the sibling embryos developed to stage 16. Then animal caps were collected for RNA extraction, and *msmb3L* expression was examined through RT-PCR. The expression of *foxd3* was a positive control to validate neural crest induction, and *odc* was used as loading control.

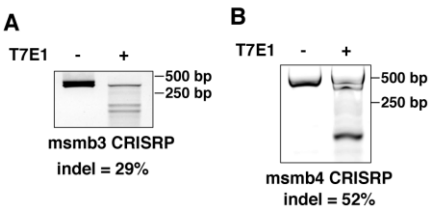

Supplementary Figure 3. The Cas9 protein and sgRNA targeting *msmb3* (A) or *msmb4* (B) were co-injected into *X. tropicalis* embryos at one-cell stage. When the embryos developed to stage 20, genomic DNA was extracted for T7E1 assay. The gene disruption efficiency for *msmb3* and *msmb4* were 29% and 52%, respectively.

Supplementary material 1

```
>Xenopus laevis msmb.3L mRNA sequence
TAGTGTCTGCAACAACTTCAAGCATAATGAAACATTTTCAGAATCTAGTTTTGGTTTCTGTGATTGCGTTTGGCCTTTTGGTAACA
TCATGTAATGCTTCCTGCGCGATTTACATTCCAGAGGTGGGAAAGATAAAAGGTTGCAAATATAAAGGCAAGCTGCACAGGTTAGG
GAGCACATTTAGAACCAAAGATTGTATGGACTGTAGCTGTGGTTTGGACGGCTCAATGGAATGTTGTCAATCATATAAGACCCCAG
TGCAGTATGATAAGGAAAAGTGTACGGCTGTTTTTTAATAAGAAAAACCTGCTCTTATCAAGTGGTGGAAAAGAAAAATCGTTCAAG
GGAATGTGACGTTTTTGCTATGGTTGGCTGAAATAGCTGTCTTCTTGGGAAAGAGCATCATGAACGGAATCCAGATCCTTATAAAC
AAAGATAAAGCAATTTGTTCAACATGAATGAATTTAACAGATAACTAAAAATAAAGTCATTAAGAGAA
```

Supplementary Table 1. Differentially expressed genes

Gene symbol	Fold change	*p*-value	Gene symbol	Fold change	*p*-value
kcnk4	8.49	0.0178	LOC100485989	34.56	0.0447
adgrl4	-22.40	0.0006	LOC100493184	9.01	0.0006
LOC101730303	32.71	0.0393	LOC101732718	9.93	0.0080
slc7a10	7.55	0.0078	LOC105947862	6.93	0.0495
fads2	-74.19	0.0027	LOC101735245	35.19	0.0467

LOC101732799	6.78	0.0394	LOC100485858	36.23	0.0007
LOC100497150	-4.75	0.0218	LOC108648114	225.62	0.0005
arsa.2	-33.25	0.0438	LOC108648059	240.66	0.0019
LOC105946844	-35.84	0.0301	LOC101731998	145.51	0.0015
kcnd2	41.30	0.0154	LOC105947943	3.28	0.0218
LOC100485706	9.53	0.0115	LOC100491292	2.03	0.0364
LOC105946797	-33.25	0.0438	LOC100487974	29.31	0.0493
LOC101731759	16.33	0.0049	ceacam20	-6.50	0.0399
LOC108645872	116.05	0.0101	LOC100493733	-2.18	0.0396
gabra5	-4.12	0.0477	tmc1	6.94	0.0199
LOC101731328	42.21	0.0169	LOC100135243	7.42	0.0306
myom3	-10.96	0.0179	LOC100498331	33.59	0.0332
tmigd1	-3.30	0.0410	nxpe1	-5.45	0.0353
LOC101732176	4.61	0.0188	LOC101733856	30.04	0.0000
LOC101732251	10.96	0.0064	LOC108648146	32.71	0.0393
LOC100496120	-3.55	0.0239	abcg4	-7.13	0.0001
LOC101735043	44.08	0.0175	cd3g	7.21	0.0328
LOC101730332	-5.76	0.0002	mpzl2	-1.77	0.0116
LOC108645501	6.30	0.0135	bace1	-2.93	0.0142
LOC100145277	4.68	0.0487	tnfrsf14	2.25	0.0293
LOC101732312	48.43	0.0103	LOC100498388	-34.21	0.0000
LOC101731297	-27.34	0.0000	LOC105946026	50.49	0.0000
LOC101735182	25.54	0.0003	LOC100491286	12.13	0.0000
LOC101734858	71.12	0.0019	mmp23b	6.88	0.0469
LOC108645444	-1.73	0.0254	tmem240	-3.87	0.0316
LOC100494837	7.05	0.0376	LOC105947805	-2.11	0.0113
LOC100498422	9.03	0.0398	ilvbl	-1.63	0.0232
LOC101731705	4.37	0.0012	LOC101734646	-5.20	0.0021
gata1	-36.46	0.0226	siae	-2.36	0.0010
LOC101732332	52.92	0.0232	barx2	13.68	0.0000
LOC100495294	5.15	0.0058	ets1	-2.59	0.0000
LOC105948036	10.97	0.0266	LOC100492897	-1.96	0.0288
LOC100496720	-3.60	0.0341	slc43a1	-6.08	0.0000
MGC89056	-1.88	0.0305	camk2g	-1.67	0.0308
LOC108645298	-35.45	0.0423	LOC108648196	10.69	0.0013
cyp2c37	-6.27	0.0485	LOC100488368	3.55	0.0105
LOC105945814	-7.91	0.0365	igsf9b	-3.86	0.0004
xa-1	-3.34	0.0105	tirap	-6.47	0.0003
edn3	-32.64	0.0333	LOC100490435	-3.05	0.0089
LOC100496865	-49.49	0.0126	LOC108648121	-45.33	0.0156
abcc8	-10.62	0.0449	LOC100497030	-3.63	0.0246
LOC105947852	2.81	0.0372	vstm4	3.20	0.0464
LOC100497187	-2.90	0.0194	wdfy4	-2.50	0.0135
ptpro	5.61	0.0468	pga4	-4.75	0.0176

LOC108645198	-6.34	0.0358	msmb.3	-2.67	0.0053
LOC108645156	37.45	0.0224	LOC100494753	2.13	0.0011
LOC101734290	-7.15	0.0296	LOC108648180	11.47	0.0054
LOC101733852	-54.62	0.0129	slc22a15.2	3.70	0.0001
LOC105946381	-6.15	0.0371	entpd1	1.80	0.0083
fcn3	-28.81	0.0508	hps1	2.16	0.0392
LOC100493719	-28.55	0.0495	ldb1	-1.46	0.0463
LOC108644786	-7.19	0.0090	LOC105947624	7.37	0.0338
LOC101730755	-39.96	0.0181	nkain3	4.11	0.0314
LOC101734537	-56.07	0.0040	aqp4	32.71	0.0393
LOC100492859	41.30	0.0154	ptprm	-1.85	0.0237
LOC105945277	46.56	0.0127	LOC105947533	89.35	0.0172
pnmt	33.59	0.0332	irf4	-44.98	0.0125
LOC100490729	-6.27	0.0485	nrn1	7.46	0.0289
cps1	-14.62	0.0005	LOC108645678	-11.03	0.0343
LOC100489851	-40.27	0.0158	LOC100492839	-3.90	0.0131
trpm2	-5.10	0.0397	LOC100494929	-3.37	0.0273
LOC108648913	5.04	0.0256	LOC101730218	-41.56	0.0263
LOC108645160	41.30	0.0154	LOC100491450	-4.03	0.0379
LOC108648772	-10.33	0.0274	cldn16	-6.96	0.0128
LOC108648877	34.56	0.0447	LOC100494190	5.20	0.0168
slc5a11	-32.07	0.0403	LOC105947297	40.83	0.0175
LOC101731224	11.08	0.0249	hmgcll1	-40.27	0.0158
LOC100492630	-6.54	0.0117	slc35d3	35.91	0.0407
LOC105947129	-32.37	0.0344	c2cd4c	-4.67	0.0094
LOC100493406	-12.44	0.0272	MGC107884	4.75	0.0242
LOC101731307	-40.85	0.0166	LOC105947361	-48.47	0.0076
sptb	-3.99	0.0293	LOC108647648	-4.16	0.0391
tnfaip2	-3.88	0.0369	LOC101734175	-6.96	0.0144
ptgdr	5.83	0.0412	c4h1orf146	-33.25	0.0438
LOC105948166	-12.44	0.0272	LOC105947290	-11.03	0.0343
map4k1	51.52	0.0101	izumo1r	13.93	0.0106
LOC100486352	11.19	0.0317	LOC105945776	6.55	0.0482
LOC108648352	-4.05	0.0323	bean1	29.31	0.0493
LOC101733426	-3.39	0.0138	LOC105947232	58.21	0.0399
tnfsf10l	-37.82	0.0474			

Supplementary Table 2. Primers and oligos used in this study.

Name	Forward Sequence (5'-->3')	Reverse Sequence (5'-->3')
	qPCR	
igsf9b	GTTATTGGCACCAGCCCTCA	AACTGGGCACGCTTTATCCA
entpd1	CCTGTTCCATCCCAGGAACC	GCACAGGGGACTTGCCTATT
nnmt	GCACAGATGCTACTCACCACT	GCTGAGTTTTGGGATCGACT

tirap	GGTCCTGTGATGACAGCGTAT	CCTTTTCTCAGTGCACATGAAGTT
ncRNA435	TTGTGCACCAGTTGATCCCT	CTCCACATCCTTGGCCACTT
ncRNA196	CCACGGCACATGGGGATAAT	AATCTTGGCTACGGTGGGTG
slc22a15	ATAGGGGAATTCGGCTGCTG	CACTGCACCGACTAAGACGA
barx2	ACATCCCCATCCTCCCATCA	ACGCCGTGGCTTTTTCATTC
foxd3	TTGAAGGTAGGCACTCGCTG	CATTCCAGCTACGGGTCCTC
snail2	CCCCATTCCTGTATGAGCGG	TGAAGCAGTCCTGTCCACAC
twist1	AGGGTCATGGCCAATGTCAG	GTTTGTCAGAGGGGAGGGTG
xt-msmb1	GCAACAACAATCTGCAACAACTG	TTTTCAGGCGGCAGATGGAA
xt-msmb2	TAAGTAGGGGGAGAGCAGGG	CACCAAAATGCCAAGGGCAA
xt-msmb3	CCGAGTTGGGAGAAGCCAAA	GGCAACATTCCATTGAGCCG
xt-msmb4	ACAGTGGCATGTCCTTGCTT	GCCACTGACCTGAAGGTTCT
xt-msmb5	AATCAGCCGCCTGAAAACCA	ATCCACTGGGGTGCCATGTA
xt-odc	AGGCCACACTGGCAACTCA	TGCGCTCAGTTCTGGTACTTCA
xl-msmb3L	TGTAATGCTTCCTGCGCGAT	ATTGAGCCGTCCAAACCACA
xl-msmb3S	AGCTGAATGTGGTCCCTGTG	CCCTTTGGATCCCGAGTGTAG
xl-odc	TGCACATGTCAAGCCAGTTC	CTACGATACGATCCAGCCCA
	subcloning	
plet1	GGCCGGATCCAGCTCTTTACCTGCTTGGGAC	GCGCGAATTCGAGTTGGGCTTCTGGCTACA
ankrd65	GGCCGGATCCTTGCATGGTCACATCTGCTTTG	GCGCTCTAGATGTCCACACACTGCTGATCTC
wdfy4	GGCCGGATCCTCGAGAGCGCAGTCAAAAGT	GGCCGAATTCTTGCTTCAGACTGCAGGGAG
tbata	GGCCGGATCCTTCCTCTGTGCTGCAGGTTC	GCGCGAATTCTGGGTTGGCAGGATGTAGTT
slc43a1	GGCCGAATTCGAATCAACGGGTACAGCAAGT	GCGCTCTAGACAGCCCAACATTATCGCCAC
ncRNA435	GGCCGAATTCTGCAAAGATCCTGACCCCTG	GCGCTCTAGACACAAAATCTTGCTGATGCACAC
ppm1h	GGCCGGATCCAGTAGCAGTGACATCCCCCT	GCGCTCTAGATGTTGCTCGAGGTGCTTTCT
slc25a16	GGCCTCTAGAGGCACCACCCAGTGTTTTTC	GCCGCTCGAGCAGCCAAACTTTCACTGGGC
p3h1	GGCCGGATCCTCAATTAGGGGAGAGCTGTGT	GCCGTCTAGAGAGTATGAGGGGAGGTTGTGC
glipr2	GGCCTCTAGATTGGGCCTTCAGGGGTATCT	GCCGCTCGAGTCTCGAGGGAAACGCTGAAC
msmb3	GGCCTCTAGATGGGCCTTTTGGTAACAGCA	GCCGCTCGAGCCCTAGCCGACCATAGCAAA
cpras1	GGCCTCTAGATCAAATGCACATGTTTCTGGTC	GCCGCTCGAGTGGAGTCATCGTCAGGAGTTC
fgf6L	GGCCGGATCCAGGGAGGATGCAAGTAGC	GCCGCTCGAGCTTGGGTATGCAGGGAGTT
	Genotyping	
xt-ets1	TCCCCGAGAATGGACAGAC	CTTTCTGTAAGATCTCCAAGTGCT
p-wt	GTGGACTTTCAGAAGTTC	
p-ko	GAAAGGAGTGGACTTTTGAG	
xt-msmb3	TGGGGGAGGGTAAAGTTACAA	TCCTCACAACCTTACCAGTTTT
xt-msmb4	TTGGCTTGTGTGATTGCCGT	TAACTGCAGAAACCCACTGTCA
	sgRNA assembly	
msmb3-TS	TAGGCTCAATGGAATGTTGCCA	AAACTGGCAACATTCCATTGAG
msmb4-TS	TAGGCTCAATGGAATGTTGCCA	AAACTGGCAACATTCCATTGAG
	ChIP	
P-msmb3L	CCCCTAGGCTTGTTATGTTTAGA	CAGGCAAGAATTGAGCAACCC
P-id3	CGGTATGTGCAATTATCTA	AAAAGCCATTATTCTGTATC
P-con	TCCACATGCACAACCCTTTA	TCTTTGCCCACAAATCTGGT